

Structural characterization of high temperature AlN intermediate layer in GaN grown by molecular beam epitaxy

A.M. Sanchez ^{a,*}, F.J. Pacheco ^a, S.I. Molina ^a, J. Stemmer ^b, J. Aderhold ^b, J. Graul ^b

^a *Departamento de Ciencia de los Materiales e I. M. y Q. I., Universidad de Cádiz, 11510 Puerto Real (Cádiz), Spain*

^b *Laboratorium für Informationstechnologie, Universität Hannover, 30167 Hannover, Germany*

Abstract

Transmission electron microscopy has been used to study the structural quality of GaN grown on sapphire by plasma assisted molecular beam epitaxy using high temperature AlN intermediate layers with different thicknesses. The introduction of an AlN intermediate layer with an optimum thickness is observed to minimize the density of dislocations reaching the overgrown GaN surface. In this sample, the measured threading dislocation density reaching the surface of $1 \times 10^{10} \text{ cm}^{-2}$ resulted to be seven times lower than that of a reference sample, without any AlN interlayer. The bending at the GaN/AlN interface and following interactions between dislocations have been observed in cross-sectional transmission electron micrographs. This fact explains the decrease of dislocation density reaching the GaN surface. © 2001 Published by Elsevier Science B.V.

1. Introduction

The development of GaN-based devices including super-bright blue and green light emission diodes and continuous wave laser diodes at room temperature has been achieved on (0001) sapphire substrates. This kind of substrate has been widely used for growth of GaN and related compounds such as AlN and InGaN. These devices own comparable efficiencies to those achieved in equivalent red-emitting GaAs-based devices in spite of the high defect densities observed in GaN layers.

As a result of the mismatch between the thermal expansion coefficients and lattice parameters of GaN and sapphire, the growth of GaN directly on sapphire leads to the formation of three-dimensional islands [1,2] and gives rise to epilayers with high dislocation density [3]. However, buffer layers are employed to promote uniform coverage of the GaN.

Although the optical properties and lifetimes of GaN-based LEDs are remarkably insensitive to dislocations [4], the high level of dislocations in GaN films limits laser [5] and microwave device performance.

The use of low-temperature buffer layers (LT-buffer) as AlN [6–8] and GaN [2,8], produces a filtering effect that reduces the threading defects in the epilayer. In

this way, the introduction of a LT-buffer layer improves the crystallinity and surface morphology of the overgrown III-Nitride layer, enhancing its electrical and luminescent properties. Recent studies have demonstrated that insertion of LT-GaN or LT-AlN interlayer between high-temperature (HT) GaN layers reduces threading dislocation densities [9]. This work evaluates and explains why the introduction of a HT intermediate AlN layer in GaN grown by plasma assisted molecular beam epitaxy (MBE) on sapphire reduces the density of threading dislocations at the surface of the grown GaN layer.

2. Experimental

A 20 nm thin GaN buffer layer was deposited by plasma assisted MBE at 580°C, followed by annealing at 750°C, on (0001) sapphire substrates, before starting growth of a GaN epitaxial layer at 685°C. A thin AlN intermediate layer (AlN-IL) was then deposited on a nominally 100 nm thick GaN layer without any growth interruption at the same temperature as GaN has been grown. At the end, a nominally 400 nm GaN layer was grown over these structures. Following this procedure, a series of three samples (T1, T2 and T3) has been grown. AlN-IL thickness for these samples was 3.2 nm (sample T2) and 8.0 nm (sample T3). Sample T1 was

* Corresponding author.

E-mail address: ana.fuentes@uca.es (A.M. Sanchez).

grown at the same conditions directly on GaN buffer layer without any AlN-IL layer and it is used as a reference sample. Further growth details on the studied samples are described elsewhere [10].

Room temperature photoluminescence (PL) measurements on all samples were performed using a HeCd laser emitting at 325 nm.

The microstructure of the layers was characterized by conventional transmission electron microscopy (TEM) in a Philips CM 20 transmission electron microscope operated at 200 kV. Thickness of the AlN-IL was measured by high resolution electron microscopy (HREM) in a Philips CM300 FEG transmission electron microscope. Plan view TEM (PVTEM) specimens were thinned down to 100 μm by mechanical grinding and dimpled down to 5 μm followed by ion milling with a LN₂ cold stage at 4.5 kV to electron transparency. Cross-sectional TEM (XTEM) samples were prepared by tripod technique. Electron transparency was achieved using PIPS (Precision Ion Polishing System) at 5 kV. A final step at 3 kV was used to reduce ion beam damage.

3. Results and discussion

The defect morphology and density of samples T1, T2 and T3 has been studied using TEM, HREM and selected area electron diffraction (SAED) techniques.

We determined the orientation relationship between GaN and sapphire substrate by SAED at different regions in the interface. The epilayer was found to have the hexagonal wurtzite crystalline structure oriented with its $[11\bar{2}0]$ parallel to the Al₂O₃- $[10\bar{1}0]$. The $[0001]$ of the epilayer and substrate coincide.

SAED patterns registered from areas of about 100 μm^2 of PVTEM specimens (Fig. 1) show the existence of a

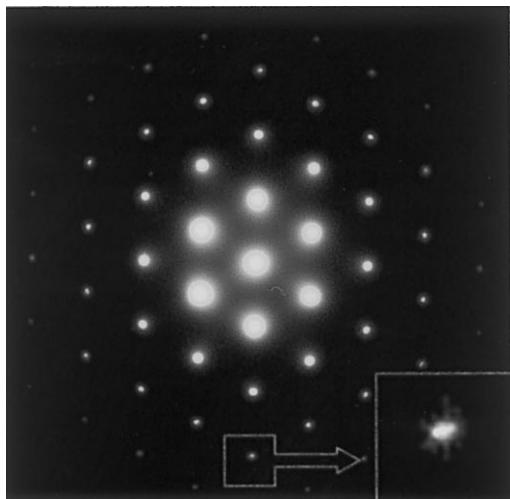


Fig. 1. $\langle 0001 \rangle$ SAED pattern of the GaN layer registered from a plan view specimen.

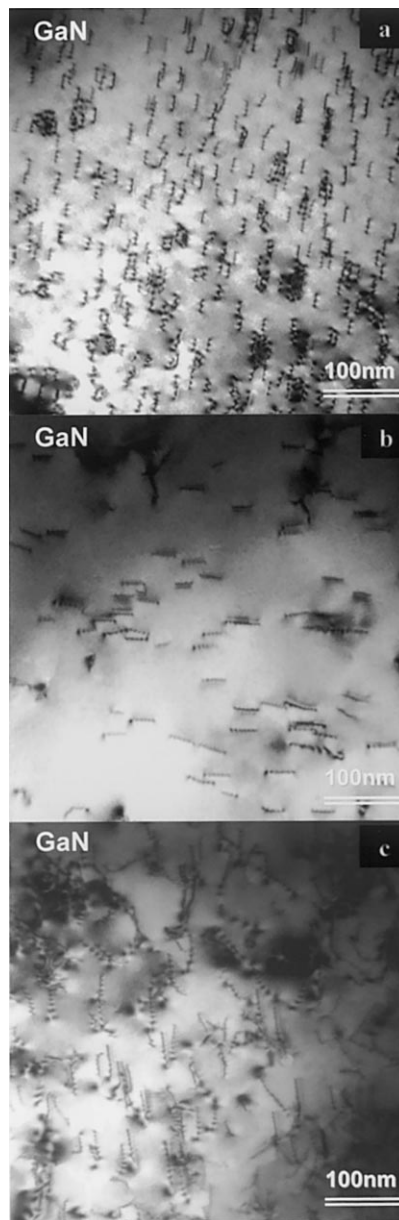


Fig. 2. Bright field PVTEM image registered under two beam conditions with $g = 11\bar{2}0$ near $\langle 1120 \rangle$ axis zone for sample (a) T1, (b) T2 and (c) T3.

very slightly in-plane misoriented structure. The elongated and curved shapes of the spots display the misorientation degree. SAED patterns were recorded in the same conditions for all samples. A similar in-plane

Table 1

Dislocation density, AlN layer thickness and PL characteristics of studied samples

Sample	T1	T2	T3
Dislocation density (10^{10} cm^{-2})	7	1	3
AlN layer thickness		3.2	8
FWHM PL (meV)	61.4	42.7	50.1
PL peak (eV)	3.420	3.431	3.443

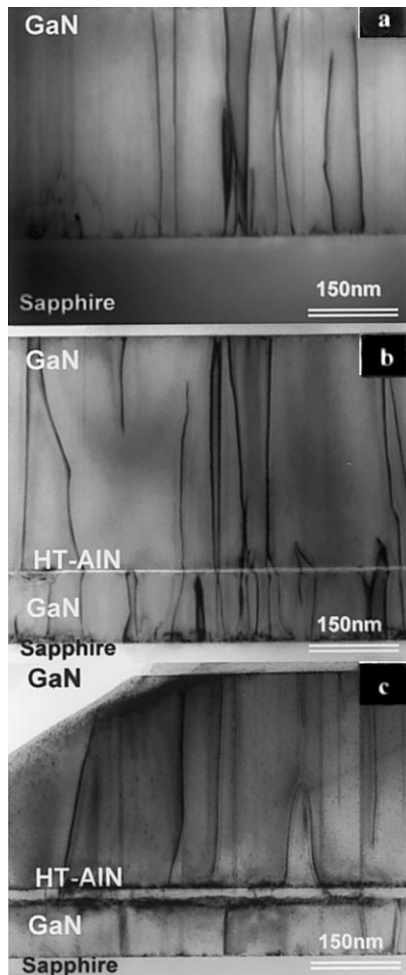


Fig. 3. Bright field XTEM image recorded under two beam conditions for $g = 0002$ near $\langle 11\bar{2}0 \rangle$ zone axis showing the dislocation line behaviour and interaction between dislocations close to the GaN/AlN interface for sample (a) T1, (b) T2 and (c) T3.

misorientation has been estimated from the registered patterns. The HT-AlN interlayer insertion does not seem to influence the mosaic structure, since the spot curvature was similar and less than 2° in samples with and without HT-AlN interlayer. The slightly curved and elongated shape of diffracted spots show that the twist misorientation, typical of films having a large lattice mismatch with their substrates [11] is less than in GaN epilayers grown over Si(1 1 1) substrates [12]. Thus, the AlN interlayer existence appears to have no influence on the GaN top layer mosaic structure.

Fig. 2 shows images taken in two beam conditions with $g = 11\bar{2}0$ for the complete series of samples. From these images recorded under the same conditions, a clear dislocation density change can be observed in series of samples T1–T3. Three types of perfect Burgers vectors can occur in wurtzite layers: $b = \langle 0001 \rangle$, $b = 1/3\langle 11\bar{2}0 \rangle$ and $b = 1/3\langle 11\bar{2}3 \rangle$. The analysis of PVTEM images (Fig. 2) registered in two beam conditions with $g = 11\bar{2}0$, permits to determine the dislocation density reaching the

surface of the overgrown GaN layer. Due to the diffraction contrast $g \cdot b$ invisibility the dislocations considered for the measured density, ρ_D , are those with Burgers vectors $b = 1/3\langle 11\bar{2}0 \rangle$ and $b = 1/3\langle 11\bar{2}3 \rangle$. Nevertheless, the dislocations with such Burgers vectors represent the majority of them in the system AlN/GaN.

In XTEM images half loops have been observed to appear without reaching the GaN surface. In previous reports (GaN/6H-SiC [13] and GaN/sapphire [14] systems), these defects, originated at the interface, were identified to have a $[0001]$ Burgers vector. Pairs of this kind of dislocation with opposite Burgers vectors tend to annihilate each other when more material is deposited during the growth. Although a small fraction of them could extend further away from the interface, and occasionally reach the surface, this fraction is negligible in relation to the dislocation density with an a -component.

In this way, the measured values of ρ_D for the different samples are summarized in Table 1. These measurements reveal a decrease in ρ_D of samples with AlN-IL (T2 and T3), compared to the reference sample (T1). Additionally, the full width at half maximum (FWHM) of the PL main emission peak of each sample is shown in the same table. The lowest dislocation density and FWHM from PL measurements were observed for sample T2.

The ρ_D decrease is related to the threading dislocations behaviour at the interface between GaN and the HT-AlN interlayer. This behaviour is different for the studied samples, as can be observed in Fig. 3. On the other hand, as can be expected, the HT-AlN interlayer thickness influences the change of dislocation line direction. Let us suppose a threading dislocation that extends from the substrate to the surface of the epitaxial film. When the film thickness exceeds a critical value, some of these straight threading dislocations change into the basal plane to become misfit segments parallel to the interface. This fact has been observed before in previous reports [15,16]. This dislocation bows and moves to the edge of the sample and escapes from it.

XTEM images of sample T2 with $g = 0002$ near the $\langle 11\bar{2}0 \rangle$ axis (Fig. 3(b)) show some dislocations bending in the AlN-IL. Most of the times these threading dislocations do not become misfit dislocation in (0001) plane. Under the influence of the misfit strain, when a threading dislocation reaches the AlN-IL, it changes the direction of the dislocation line. According to this fact, interactions between bent dislocations occur, explaining the lowest values of (i) the dislocation density at the GaN surface and (ii) FWHM of the main emission PL peak of this sample.

The dislocations behaviour observed in sample T3 differ from the one described above (Fig. 3(c)). Some threading dislocations move forming half-loops across the HT-AlN interlayer, keeping nearly upright along the overgrown GaN without interactions with other dislocations.

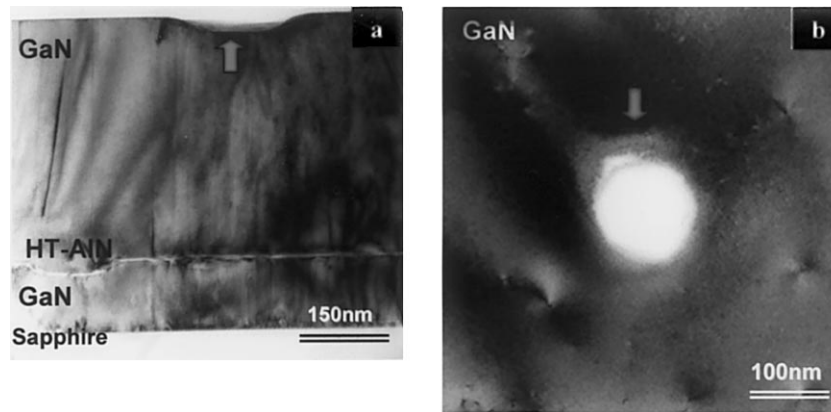


Fig. 4. Nanopipes in (a) cross-sectional and (b) planar view images for sample T2. Arrows indicate one of these defects observed from both perpendicular orientations.

The AlN-IL in sample T2 and T3 was studied by HREM. The interlayer thickness was measured by $\langle 11\bar{2}0 \rangle$ HREM images analysis. Nevertheless, the interlayer is not abrupt along the whole interface but there are a few thicker regions in AlN-IL. This explains that misfit segments originated from threading dislocations were not present uniformly in the sample.

Fig. 4(a) shows an XTEM (0002)-bright field image, taken near $\langle 11\bar{2}0 \rangle$ axis orientation. Only dislocations with Burgers vectors $b = 1/3\langle 11\bar{2}3 \rangle$ and $b = \langle 0001 \rangle$ can be observed with this reflexion.

Many of these dislocations arise straight from the first GaN layer in samples T2 and T3, before reaching the AlN interlayer. If the dislocations had $b = \langle 0001 \rangle$ and a straight dislocation line, it would lie on the $\{1\bar{1}00\}$ prism planes and it would tend to form half loops [13,14]. The other possibility is that the dislocation line had a mixed Burgers vector $b = 1/3\langle 11\bar{2}3 \rangle$. In this case it could be lying on two plane families, $\{1\bar{1}01\}$ and $\{2\bar{1}\bar{1}2\}$. The Peierls force acting on dislocations in slip systems with a large Burgers vector, $\langle 0001 \rangle$ (c-type) or $b = 1/3\langle 11\bar{2}3 \rangle$ (a + c-type) is very high. In spite of the large Peierls force in these slip systems, $1/3\langle 11\bar{2}3 \rangle\{10\bar{1}1\}$ and $1/3\langle 11\bar{2}3 \rangle\{2\bar{1}\bar{1}2\}$, they are the unique possibilities for these straight dislocations with $b = 1/3\langle 11\bar{2}3 \rangle$. The Peierls force acting in the $b = 1/3\langle 11\bar{2}3 \rangle\{10\bar{1}1\}$ system is lower than in $b = 1/3\langle 11\bar{2}3 \rangle\{2\bar{1}\bar{1}2\}$, so in principle for these dislocations it is more likely to be lying in $\{10\bar{1}1\}$ planes.

AlN-IL thickness of sample T2 would not exceed the critical value, so the threading dislocations would not bend to form half-loops across the interface, but the influence of misfit strain changes the line direction. If the interlayer thickness was larger than this critical thickness in different regions of the sample, the threading dislocations could provide misfit dislocation segments. This segment will move along $\langle 11\bar{2}0 \rangle$ direction, and so it will form a 60° misfit dislocation with the Burgers vector projection. In sample T3 the probability to find misfit

segments formed from threading dislocations with $b = 1/3\langle 11\bar{2}3 \rangle$ is higher because the AlN-IL thickness would exceed the critical value for this system.

Images recorded under two beam condition with $g = 0002$ near $\langle 11\bar{2}0 \rangle$ axis (Fig. 4(a)) show a smoothless surface for sample T2. From images in bright field in $\langle 0001 \rangle$ axis zone (Fig. 4(b)) we checked that many holes appeared reaching the surface. The hole size measured in PVTEM images was in the 100–200 nm range. Such holes are likely to be related to the defects named “nanopipes”. They are observed to appear at the upper HT-AlN/GaN interface. These measurements are in good agreement with the size for the defects observed by XTEM images. In the bibliography, there are many reports about hollow tubes or “nanopipes” [14,17]. This kind of defect lies closely parallel to the c -axis. The “nanopipes” often appear empty or full with amorphous material. Nearly all of the observed nanopipes are associated to screw dislocations [18].

4. Summary

The introduction of a thin AlN intermediate layer in a GaN layer grown by plasma assisted MBE on sapphire (0001) reduces the density of threading dislocations by an order of magnitude with respect to a similar sample without any intermediate layer. This reduction of threading dislocations is associated with a clear decrease of the PL peak FWHM. The optimum thickness of the intermediate layer is below the critical thickness. The value of such optimum thickness is predicted considering the bending and further interactions between threading dislocations after crossing the interfaces between GaN and the inserted AlN intermediate layer. We propose the introduction of several stacked thin AlN intermediate layers separated by GaN to strongly decrease the density of threading dislocations reaching the surface of GaN grown by plasma assisted MBE on sapphire (0001).

Acknowledgements

We acknowledge support from CICYT, Project MAT 98-0823, from the Junta de Andalucía under group TEP-0120, and are grateful to Prof. P.A. Buffat for providing TEM facilities at CIME, EPFL, Lausanne.

References

- [1] H. Amano, N. Sawaki, I. Akasaki, Y. Toyoda, *Appl. Phys. Lett.* 48 (1998) 415.
- [2] S. Nakamura, *Jpn. J. Appl. Phys.* 30 (1991) L1705.
- [3] C. Stampfl, C.G. Van del Valle, *Phys. Rev. B* 57 (1998) R15052.
- [4] S.D. Lester, F.A. Ponce, M.G. Craford, D.A. Steigerwald, *Appl. Phys. Lett.* 66 (1996) 1249.
- [5] S. Nakamura, M. Senoh, S. Nagahama, N. Iwasa, T. Matushita, T. Mukai, *MRS Internet J. Nitride Semicond. Res.* 4S1 (1999) G1.1.
- [6] S. Yoshida, S. Misawa, S. Gonda, *Appl. Phys. Lett.* 42 (1983) 42.
- [7] H. Amano, N. Sawaki, I. Akasaki, Y. Toyoda, *Appl. Phys. Lett.* 48 (1986) 353.
- [8] E.C. Piquette, P.M. Bridger, R.A. Beach, T.C. MacGill, *MRS Internet J. Nitride Semicond. Res.* 4S1 (1999) G3.77.
- [9] M. Iwaya, T. Takenchi, S. Yamaguchi, C. Wetzel, H. Amano, I. Akasaki, *Jpn. J. Appl. Phys.* 37 (1998) L316.
- [10] J. Stemmer, F. Fedler, H. Klausung, D. Mistele, T. Rotter, O. Semchinova, J. Aderhold, J. Graul, A.M. Sanchez, F.J. Pacheco, S.I. Molina, M. Fehrer, D. Hommel, *J. Crystal Growth* 216 (2000) 15.
- [11] V. Strikant, J.S. Speck, D.R. Clarke, *J. Appl. Phys.* 82 (1997) 4286.
- [12] S.I. Molina, A.M. Sánchez, F.J. Pacheco, R. García, M.A. Sánchez-García, E. Calleja, *Phys. Sta. Sol.* 176 (1999) 401.
- [13] F.R. Chien, X.J. Ning, S. Stemmer, P. Pirouz, M.D. Bremsery, R.F. Davis, *Appl. Phys. Lett.* 68 (1996) 2678.
- [14] J.L. Rouviere, M. Arley, B. Daudin, G. Feuillet, O. Briot, *Mater. Sci. Eng.* B50 (1997) 61.
- [15] S. Ruminov, Z. Liliental-Weber, T. Suski, J.W. Ager III, J. Washburn, J. Drueger, C. Kisielowski, E.R. Weber, H. Amano, I. Akasaki, *Appl. Phys. Lett.* 69 (1996) 990.
- [16] B. Jahnen, M. Albrecht, W. Dorsch, S. Christiansen, H.D. Strunk, D. Hanser, R.F. Davis, *MIJ-MRS* 1 16, *Appl. Phys. Lett.* 69 (1996) 990.
- [17] D. Cherns, W.T. Young, F.A. Ponce, *Mater. Sci. Eng.* B50 (1997) 76.
- [18] W. Qian, M. Skowronski, K. Doverspike, L.B. Rowland, D.K. Gaskill, *J. Cryst. Growth* 151 (1995) 396.